Taylor & Francis
Taylor & Francis Group

Conserved charged amino acids are key determinants for fatty acid binding proteins (FABPs)-membrane interactions. A multi-methodological computational approach

Fernando Zamarreño[a], Alejandro Giorgetti[b] ◉, María Julia Amundarain[a], Juan Francisco Viso[a], Betina Córsico[c] and Marcelo D. Costabel[a]* ◉

[a]*Departamento de Física, Grupo de Biofísica – UNS, IFISUR, Universidad Nacional del Sur, CONICET, Bahía Blanca, Argentina;* [b]*Department of Biotechnology, Faculty of Mathematical, Physical and Natural Sciences, University of Verona, Verona, Italy;* [c]*Facultad de Ciencias Médicas, Instituto de Investigaciones Bioquímicas de La Plata (CONICET-UNLP), Universidad Nacional de La Plata, La Plata, Argentina*

Based on the analysis of the mechanism of ligand transfer to membranes employing *in vitro* methods, Fatty Acid Binding Protein (FABP) family has been divided in two subgroups: collisional and diffusional FABPs. Although the collisional mechanism has been well characterized employing *in vitro* methods, the structural features responsible for the difference between collisional and diffusional mechanisms remain uncertain. In this work, we have identified the amino acids putatively responsible for the interaction with membranes of both, collisional and diffusional, subgroups of FABPs. Moreover, we show how specific changes in FABPs' structure could change the mechanism of interaction with membranes. We have computed protein–membrane interaction energies for members of each subgroup of the family, and performed Molecular Dynamics simulations that have shown different configurations for the initial interaction between FABPs and membranes. In order to generalize our hypothesis, we extended the electrostatic and bioinformatics analysis over FABPs of different mammalian genus. Also, our methodological approach could be used for other systems involving protein–membrane interactions.

Keywords: fatty acid binding protein; electrostatic interaction; molecular dynamics; protein–membrane interaction

1. Introduction

Fatty acid-binding proteins (FABPs) are intracellular proteins expressed in almost all animal tissues in different isoforms. It was proposed that they transport and target fatty acids (FA) to specific membranes or metabolic pathways. Moreover, several studies have suggested that different FABPs have unique functions and this specificity may be driven, in part, by the kind of protein–membrane interactions (Bass, 1985; Storch & Corsico, 2008; Storch & McDermott, 2009).

Structurally, FABPs are proteins of approximately 14 kDa of molecular weight with low amino acid sequence homology among different members of the family, but sharing a common tertiary structure consisting of 10 antiparallel β-strands that form a β-barrel, which is capped by two short α-helices arranged as a helix-turn-helix segment (Banaszak et al., 1994; Zhang, Lucke Baier, Sacchettini, & Hamilton, 2003). It is proposed that FABPs may serve not only to deliver long-chain fatty acids to target surfaces, but also to remove membrane-bound fatty acids, and this may require the direct interaction of apo-FABPs with acceptor membranes and ligand donor (Davies, Hagan, & Wilton, 2002; Storch & Thumser, 2000). The importance of electrostatics in the interaction between proteins and biological membranes has been established more than a decade ago (Neves-Petersen & Petersen, 2003). Specifically, the role of electrostatics in FABPs and biological membranes interaction was decribed in several works (Córsico, Franchini, Hjsu, & Storch, 2005; Smith & Storch, 1999; Herr, Aronson, & Storch, 1996; Zamarreño, Herrera, Córsico, & Costabel, 2012). Moreover, it has been shown that specific mutations could interfere in the process (Davies et al., 2002; Falomir-Lockhart, Laborde, Kahn, Storch & Córsico, 2006; Liou & Storch, 2001), but the precise mechanism of this interaction, and the structural regions of the protein responsible for driving the interaction and possibly determine different binding mechanisms between FABPs and membranes, remain unknown. *In vitro* studies have shown that different FABPs transfer fatty acids to phospholipid membranes employing two different mechanisms. Most FABPs, including intestinal (IFABP), brain (BFABP), adipocyte (AFABP), and heart (HFABP) types, transfer their FAs

by directly interacting with membranes (collisional FABPs), where the rate limiting step in the transfer process is the interaction of the protein with the membrane. In marked contrast, other members of the family, as liver FABP (LFABP), transfer their ligands to and from membranes by a supposed aqueous-diffusion mediated mechanism (diffusional FABPs), where the rate limiting step in the transfer process is the liberation of the ligand from the protein binding site (Herr, Li, Weinberg, Cook, & Storch, 1999; Hsu & Storch, 1996; Storch & Thumser, 2000; Storch & McDermott, 2009; Thumser, Tsai, & Storch, 2001).

Several experimental studies have provided substantial evidence describing IFABP interaction with membranes, and have shown that electrostatic and hydrophobic forces modulate these physical interactions (Falomir-Lockhart et al., 2006; Falomir-Lockhart, Franchini, Guerbi, Storch, & Córsico, 2011; Franchini, Storch, & Córsico, 2008; Hsu & Storch, 1996; Thumser et al., 2001). In contrast, LFABP has been classically considered a 'diffusional' FABP, based on FA transfer kinetic studies (Hsu & Storch, 1996; Thumser & Storch, 2000). More recent studies which analyzed I- and LFABP's capacity to directly interact with membranes, employing different experimental approaches, have shown that LFABP is also able to interact with phospholipid membranes (Ceccon, Lelli, D'Onofrio, Molinari, & Assfalq, 2014; Falomir-Lockhart et al., 2011). It was also demonstrated that the factors that modulate this process are different for each protein, implying different roles for IFABP and LFABP in an intracellular context.

To get insight into the mechanism of the interaction between FABPs and membranes, in a previous work, we modeled this process *in silico*. Indeed, we have computed the protein–membrane interaction energies for several members of the family with membranes. We showed that binding of FABPs to membranes involves a significant electrostatic component that discriminates among possible membrane-bound mechanisms and we classified a list of FABPs according to the interaction mechanism (Zamarreño et al., 2012). The proposed classification and the results of this model are in total agreement with experimental observations for FABP-membrane interaction (Storch & McDermott, 2009; Storch & Thumser, 2000). Furthermore, our results are in concordance with Molecular Dynamics simulations that have shown different configurations for the initial interaction between FABPs and membranes (Friedman, Nachliel, & Gutman, 2006; Mihalovic & Lazaridis, 2007; Villarreal, Perduca, Monaco, & Montich, 2008).

In the present work, we have identified the amino acids putatively responsible for both, collisional and diffusional, mechanisms; and, show how specific changes in FABPs' structure could change the mechanism of interaction with membranes. Due to the large amount of

empirical information available for rat IFABP (PDB ID: 1IFB) and rat LFABP (PDB ID: 2JU3), these two proteins were chosen as representatives for collisional and diffusional groups, respectively. In these structures we performed mutations of highly conserved charged amino acids as well as others that have been pointed as relevant for the interaction in previous publications (Davies et al., 2002; Falomir-Lockhart et al., 2006). The electrostatic energy of the interaction was calculated with modeled biological membranes. Lately, these interactions were also modeled by Molecular Dynamics (MD). Finally, we extended the electrostatic and bioinformatics analysis over FABPs of different mammalian genus, in order to generalize our hypothesis.

In a broader context, the results presented in this work set the framework for future studies directed to elucidate the precise mechanisms by which different FABPs – or other LBPs related to the family – are involved in membrane targeting. On this regard, the study of chicken liver bile acid-binding protein (LBABP) (Villarreal et al., 2008), rat IFABP (Mihalovic & Lazaridis, 2007), and ReP1-NCXSQ FABP (Galassi, Villarreal, Posada, & Montich, 2014) showed the importance of the electrostatic interactions to determine the preferred orientation of the proteins.

2. Materials and methods

2.1. Sequence analysis

Curated mammalian FABP sequences were retrieved from the Uniprot database (UniProt Consortium, 2015). The extracted sequences from five different species, including LFABP, IFABP, AFABP, HFABP, TFABP, EFABP amounts to a total of 34 sequences. Mammalian genera were chosen based on their extensive use in laboratory research, availability in protein database, and relevance for human biology (Table 1). A multiple sequence alignment was carried out using PROMALS (Pei & Grishin, 2007) with default parameters. Analysis, visualization, and pictures were carried out using the Jalview program (Waterhouse, Procter, Martin, Clamp, & Barton,

Table 1. FABPs from different tissues and species used in this work.

| Protein | Species | | | | |
	Rat	Human	Mouse	Pig	Bovine
LFABP	2JU3	2PY1	Modeled		
IFABP	1IFB	1KZW			
AFABP	Modeled	3Q6L	3HK1	Modeled	
HFABP		1G5W	Modeled		1BWY
BFABP		1JJX	Modeled		
TFABP	Modeled			Not available	Modeled
EFABP	Modeled	1B56	4AZO	Modeled	

2009). The evolutionary history of the protein family was inferred using the Maximum Likelihood method based on the JTT matrix-based model (Jones, Taylos, & Thornton, 1992). Initial tree(s) for the heuristic search were obtained automatically by applying Neighbor-Join and BioNJ algorithms to a matrix of pairwise distances estimated using a JTT model, and then selecting the topology with superior log likelihood value. The tree is drawn to scale, with branch lengths measured in the number of substitutions per site. The analysis involved 34 amino acid sequences. All positions containing gaps and missing data were eliminated. There were a total of 125 positions in the final data-set. Evolutionary analyses were conducted in MEGA6 (Tamura, Stecher, Peterson, Filipski, & Kumar, 2013).

2.2. Models and computational procedure

FABP atomic coordinates were obtained from RCSB Protein Data Bank (Berman et al., 2000) - PDB IDs: 1KZW, 2PY1, 1G5 W, 3Q6L, 1JJX, 1B56, 1BWY, 1IFB, 2JU3, 3HK1 and 4AZO-. For those proteins with unreported tertiary structure, homology models were built. The multiple sequence alignments built in section 2.1 were used for the creation of a Hidden Markov profile (HMM) of the family. The latter (for each modeled protein) was then funneled through the HHsearch (Moult, Pedersen, Judson, & Fidelis, 1995) program to identify the most plausible homologous structural templates (server's default parameters were used). We then built 15 different conformations of each target based on each of the eight structural templates using Modeller9v3 (Eswar et al., 2006), by randomizing the initial structures and optimizing by conjugate gradients and simulated annealing. Finally, model validation was performed using PROCHECK software package (Laskowski et al., 1993).

Mutant FABPs were obtained using Coot package (Emsley & Cowtan, 2004) followed by an energy minimization with GROMACS as explained below.

Equilibrated atomic coordinates for the membrane were chosen among representative structures from molecular dynamics procedures (see below). As a single component of the neutral membrane, we used 1-palmitoyl-2-oleoyl-phophatidylcholine (POPC) and anionic forms of membranes were utilized with a mix of POPC and 1-stearoyl-2-oleoyl-phosphatidylserine (SOPS). We have already shown that this technique allowed us to build several membranes with different lipid content (Zamarreño et al., 2012). For the present work a 50% POPC–50% SOPS membrane was built.

In all cases, a previous work protocol was used (Zamarreño et al., 2012): (a) Coarse grained (CG) bilayer assembly: in order to create an unbiased bilayer with a random distribution of the lipids, a CG representation of the molecules was used. (b) Final CG bilayer

construction: Once the bilayer was assembled, the system was replicated producing 200 lipids bilayer and then rotated around Y axis in order to obtain a 400 symmetric CG lipids surrounded by 6000 CG water molecules. (c) CG bilayer equilibration: 1.5 ms coarse grained molecular dynamics simulation was performed in order to ensure the correct equilibration of the coarse grained bilayer. (d) Atomistic bilayer construction: Atomistic representation of the bilayer from the coarse grained ones (reverse transformation) were obtained and minimized using a modified version of GROMACS (Rzepiela et al., 2010).

The system composed of FABP and membrane was mapped onto a three-dimensional lattice, in which the corner of each cubic cell represents a small region of the protein, membrane, or solvent. Given that the Debye Length (λ_D) for this system is 10 Å, we choose a grid extending 1.3 λ_D from either side of the system, obtaining a grid of 86 Å × 86 Å × 160 Å. The position of the grid was fixed, allowing proper cancelation of self energy electrostatic terms. Protein and membrane atomic models were considered as rigid bodies with explicit atomic details, whereas water and ions were modeled together as a continuum structureless medium. In this way, internal degrees of freedom (i.e. flexibility of lateral chains and chemical reactions) were not taken into account.

The electrostatic potential at boundary was set to the values prescribed by a Debye–Huckel model for a single sphere with radius and charge corresponding to those of the protein.

Equal amount of sodium and chloride ions (opposite and equal charges with a radius of 2 Å) was distributed linearly into the solvent cage up to 150 mM concentration. Accessible surface area and volumes were calculated using the algorithm and parameters given by Lee and Richards (1971).

The dielectric constants of lattice points located within and outside the molecular surface of the protein and membrane were set to 2.0 and 78.5 D, respectively. Ions were excluded from a region that extends 2 Å from the van der Waals surfaces of the protein and membrane. The electrostatic potential at each lattice point was calculated by solving the linear Poisson–Boltzmann equation numerically with the Adaptive Poisson Boltzmann Solver (APBS) program, which implements a PMG algorithm (Baker, Sept, Joseph, Holst, & McCammon, 2001; Holst & Saied, 1993, 1995; Lee & Richards, 1971).

2.3. Electrostatic energy difference

The solutions of the Poisson–Boltzmann equation were used to calculate the total electrostatic energy of the system (Gilson & Honig, 1988). The electrostatic interaction energy, ΔE, is the difference between the electrostatic
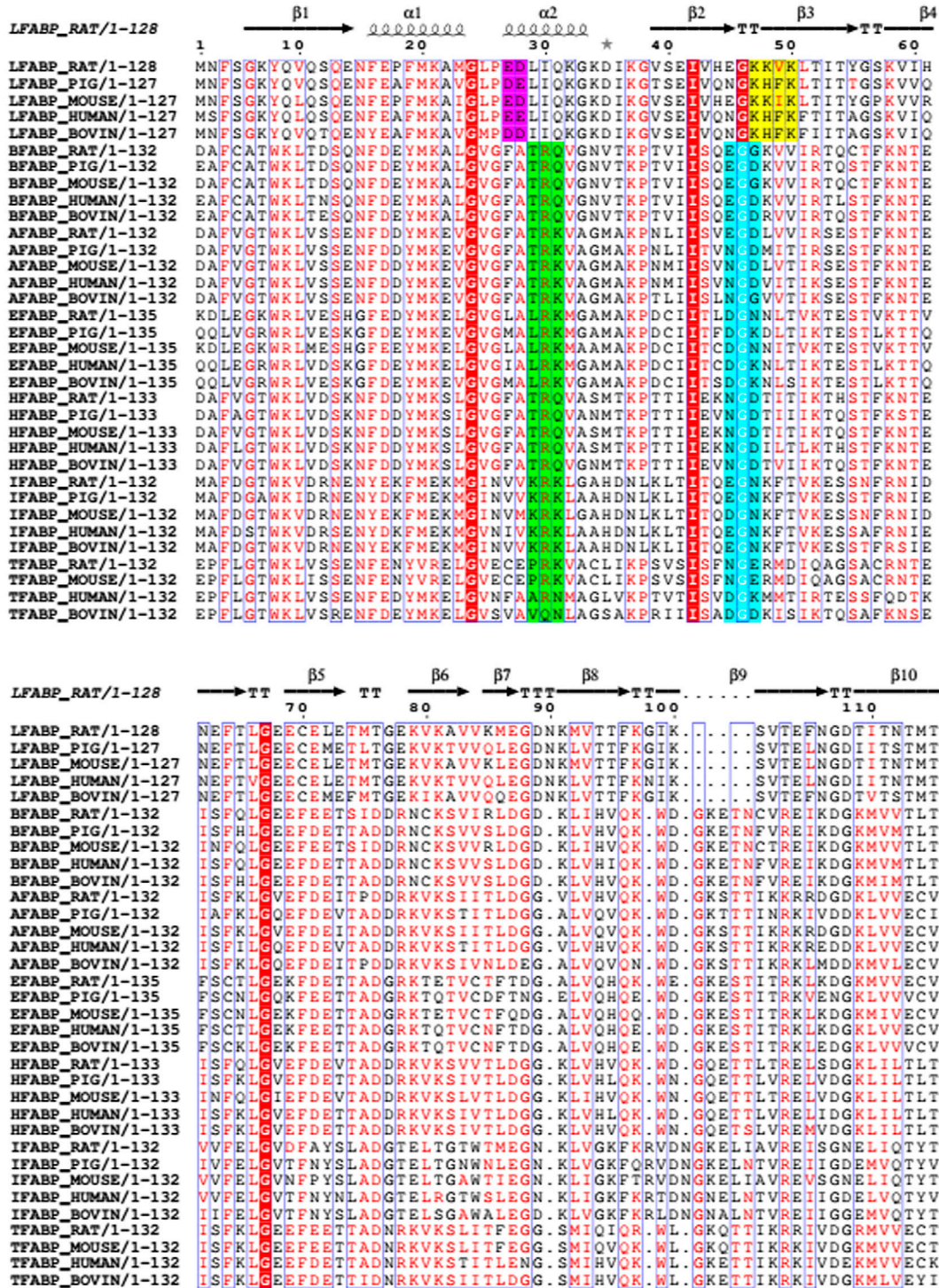
Figure 1.   Alignment of different FABPs from several mammalians sources. Although charge residues are distributed all around protein surface in different FABPs, conserved amino acids could be suitable to determine the signaling. Informative residues are defined as those conserved within the subfamilies, but variable along the whole alignment (highlighted residues). Negative/positive amino acids in helix region for diffusional/collisional FABPs (purple/green). Negative/positive zones in beta barrel region for diffusional/collisional FABPs (yellow/cyan).

energy of a system compound by FABP and membrane, and the electrostatic energy calculated for both, FABP and membrane, individually $(\Delta E = E(\text{prot} + \text{mem}) - E(\text{prot}) - E(\text{mem}))$.

Rigid bodies are located and oriented in space by a Cartesian coordinate system. Euler angles, φ, θ, ψ, describe rotations of the protein; r represents minimum distance between protein and membrane, measured from the van der Waals surface; while x and y represent translations in the plane of the membrane. We assume that a minimum in ΔE corresponds to a preferred configuration. Energy contributions other than those calculated by the Poisson–Boltzmann equation were neglected.

2.4. Sampling the electrostatic energy landscape

To calculate the membrane–protein global interaction energy for all possible configurations, we used an own developed software. This program massively generates files in PQR-format for different positions of the protein–membrane system, and these files serve as input for the APBS program. Automation and processing of data before, between, and after running the programs were carried out with Bash scripting languages.

The program varies distance and Euler angles and so we can tabulate $dE(r, \varphi, \theta, \psi)$ function. For the orientation angle increments, we sample the configuration space at intervals of $\Delta\varphi = \Delta\theta = \Delta\varphi = 45°$ $(0° < \varphi < 360°)$, $(0° < \theta < 180°)$ $(0° < \psi < 360°)$, resulting in 256 different relative positions. For relative distance between FABP and membrane we elected 3.5 Å according to values determined previously (Zamarreño et al., 2012).

It is important to point that energy value for a given set of angles will always be the same, but the shape of the curve, and consequently the appearance of minima, will depend on how we choose to sort the angles in x axis. To avoid this inconvenient, we start all calculations at the same relative position for different FABPs, ensuring that the obtained curves are comparable one to each other.

To show that minimum energy relative position is independent of how we sort the angles, and that different rotamers of residues from FABPs would not significantly affect the shape of the curve and the ΔE of the systems, we calculate ΔE for 10 different NMR models of the same FABP starting from a different set of angles than in the rest of the work (Supporting Information. Figure A).

2.5. Molecular dynamics of FABP-membranes first steps interaction

The Molecular Dynamics simulations were performed using GROMACS, version 4.5.6 (Pronk et al., 2013), with the GROMOS 53a6 force field, with Berger
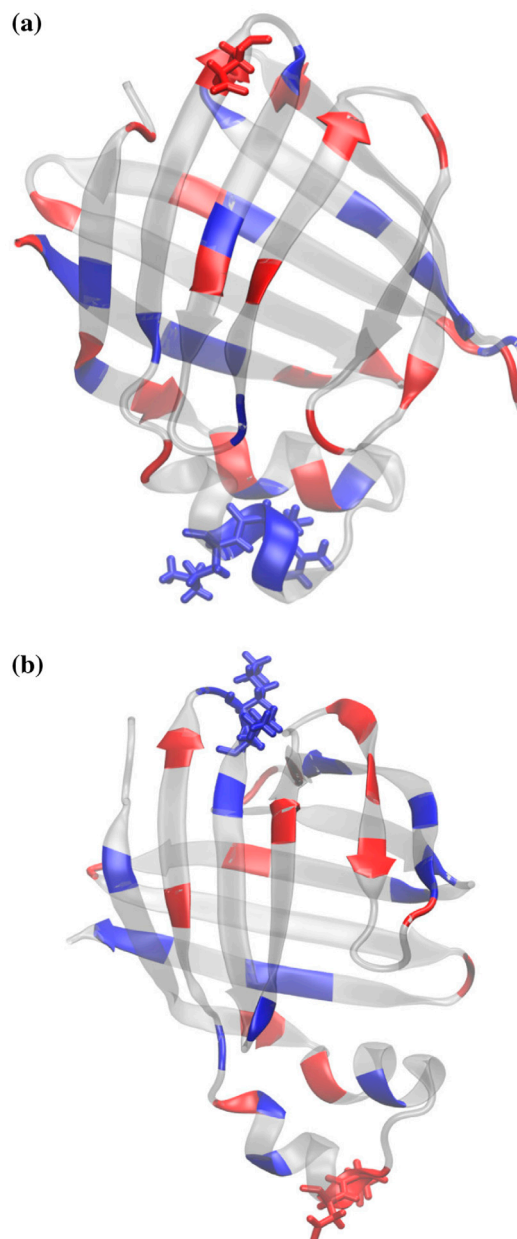

Figure 2. Charged residues in FABPs. Distribution of positive (blue) and negative (red) amino acids in Intestinal (2(a)) and Liver (2(b)) FABPs. In (a), residues 28–30 (blue sticks) of the alpha helix 2 region, and negative residue 44 (red sticks) at the opposite end of the protein of rat IFABP are indicated. In (b), negative residues 26–27 (red sticks) and residues 46–47 (blue sticks), of rat LFABP are shown.

modification for lipids (Poger, van Gunsteren, & Mark, 2010). The calculations were carried out using the structure of the apo-IFABP and apo-LFABP. Mutant proteins were obtained from these structures as described below.

The protein and membrane were embedded in a cubic box containing SPC model water (Berendsen, Postma, van Gunsteren, & Hermans, 1981) that extended

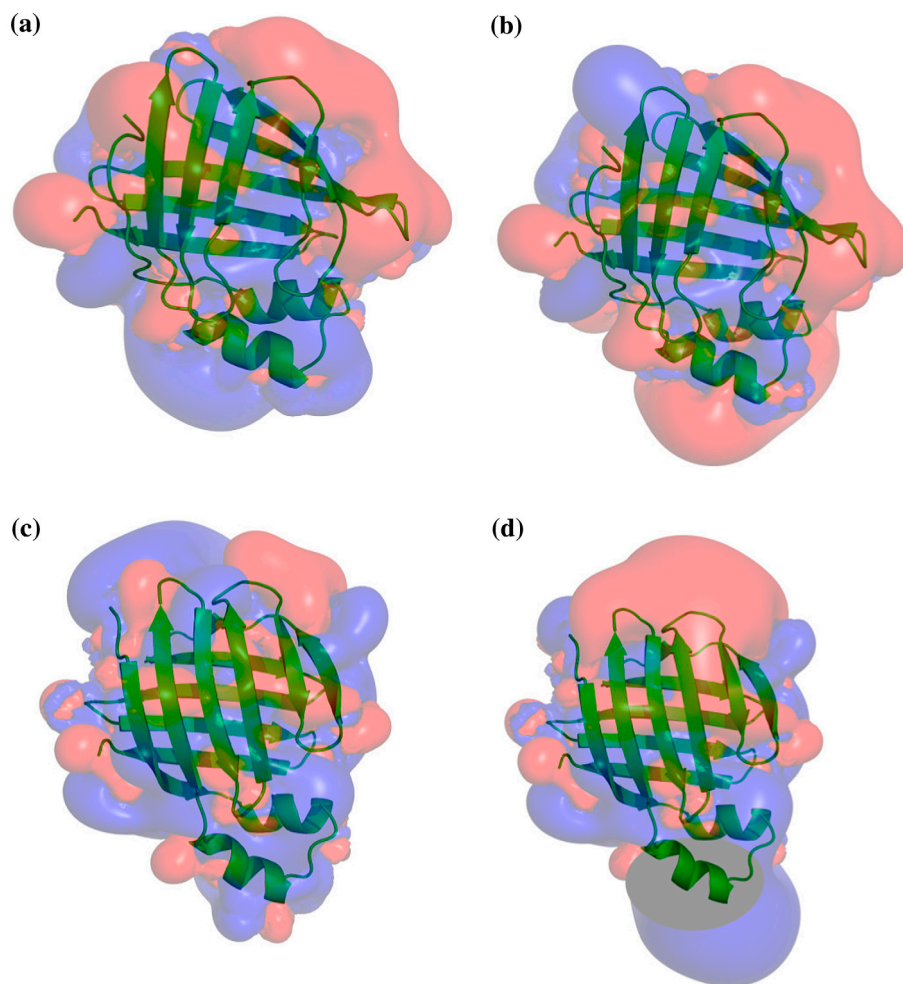**(a)**　　　　　　　　　　　　　　**(b)**

(c)　　　　　　　　　　　　　　**(d)**

Figure 3.　Charge distribution Isosurfaces for FABPs. Graphics shows the isosurfaces surrounding the molecules. Blue correspond to positive (+1), while red correspond to negative (–1) equipotential energy surfaces due to charge distribution. (a) Wild type rat IFABP. (b) Mutated rat IFABP R29E_K30E_E44K. (c) Wild type rat LFABP. (d) Mutated rat LFABP E26K_D27K_K46E_K47E.

to at least 10 Å between the protein and the edge of the box. Membrane was allowed to reach the edges of the *xy* plane, in order to simulate a continuous membrane. At the z axis, same precautions than for protein was taken, leaving at least a 10 Å distance to the edge of the simulation box.

In all cases, different amounts of Na^+ and Cl^- were added to the system by replacing water molecules in random positions, making the whole system neutral.

Before each MD simulation, energy minimizations were carried out to ensure that the system has no steric clashes or inappropriate geometry. After the minimization, MD run was performed at increasing temperatures, to avoid an abrupt reordering of the system. First 1000 ps were run at 100 K°, next 1000 ps at 200 K°, following by 1000 ps at 300 K° and finally, 17,000 ps at

310 K°. In all cases, Berendsen's thermostat (Berendsen, Postma, van Gunsteren, DiNola, & Haak, 1984) with time constant of 0.2 ps was used.

Pressure of 1 bar was simulated using Berendsen's barostat (Berendsen, et al. 1984) in an anisotropic way and with a time step of 2.0 ps. Van der Waals forces were treated using a cutoff of 12 Å. Long-range electrostatic forces were treated using the particle mesh Ewald method (Kolafa & Perram, 1992) with the following parameters: Fourierspacing = 0.12; pme_order = 4; ewald_rtol = $1e^{-5}$. The coordinates were saved every 10 ps.

Eight different simulations were run for rat IFABP and LFABP. Initial configurations for each simulation were selected according to minimum and maximum ΔE electrostatic energy for each FABP-membrane relative position.
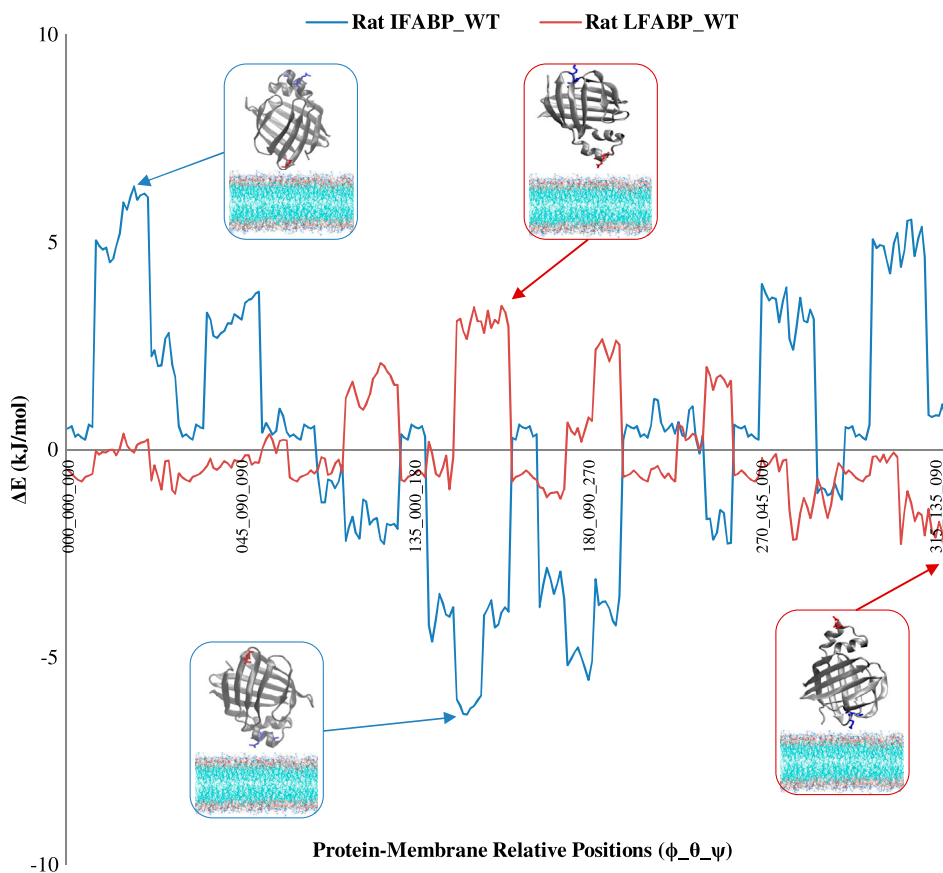
Figure 4. Electrostatic free energy versus 256 different configurations of rat wild type IFABP-membrane complex (blue line) and LFABP-membrane complex (red line). Cartoon representations of rat IFABP (blue box) and LFABP (red box), show representative protein–membrane relative position corresponding for that *x* value.

3. Results

To determine the role of specific amino acids in the interaction between FABPs and biological membranes, we used several tools of computational analysis, in an independent and sequential form:

3.1. Alignment and phylogenetic tree

The tree clearly shows a net separation of the collisional and diffusional FABPs. Collisional cluster consist in IFABP, AFABP, BFABP, HFABP (highlighted in red in Supporting Information Figure B), while diffusional cluster consists only in LFABPs (highlighted in blue in Supporting Information Figure B). The character-based algorithm used in the generation of the trees allowed us to identify the 'informative' alignment positions that putatively define the collisional/diffusional characteristics of FABPs. Informative positions are defined as those highly conserved within the subfamilies, but variable along the whole alignment. Although charged residues are distributed all over the protein surface in different

FABPs, conserved amino acids located in the helix region and in the opposite zone, i.e. in the beta barrel, would be suitable for determining the signaling (Figure 1). Thus, we have concentrated our attention principally on residues located either in alpha helix 2 or at the bottom of the beta-barrel, regions already shown to be putatively involved in protein–membrane interactions (Davies et al., 2002; Franchini et al., 2008; Zamarreño et al., 2012).

While in collisional FABPs a group of conserved positive residues are located in alpha helix 2 and conserved negatively charged ones are at the bottom of the beta-barrel (Figure 2(a)). For diffusional FABPS the situation is slightly different although equivalent. Highly conserved negative residues are located in alpha helix 2, while highly conserved positives residues are located at the bottom of the beta-barrel (Figure 2(b)). These observations prompted us to establish a virtual protocol in which conserved charged amino acids located in alpha helix 2 and at the bottom of the beta barrel, are mutated into residues with opposite charge.
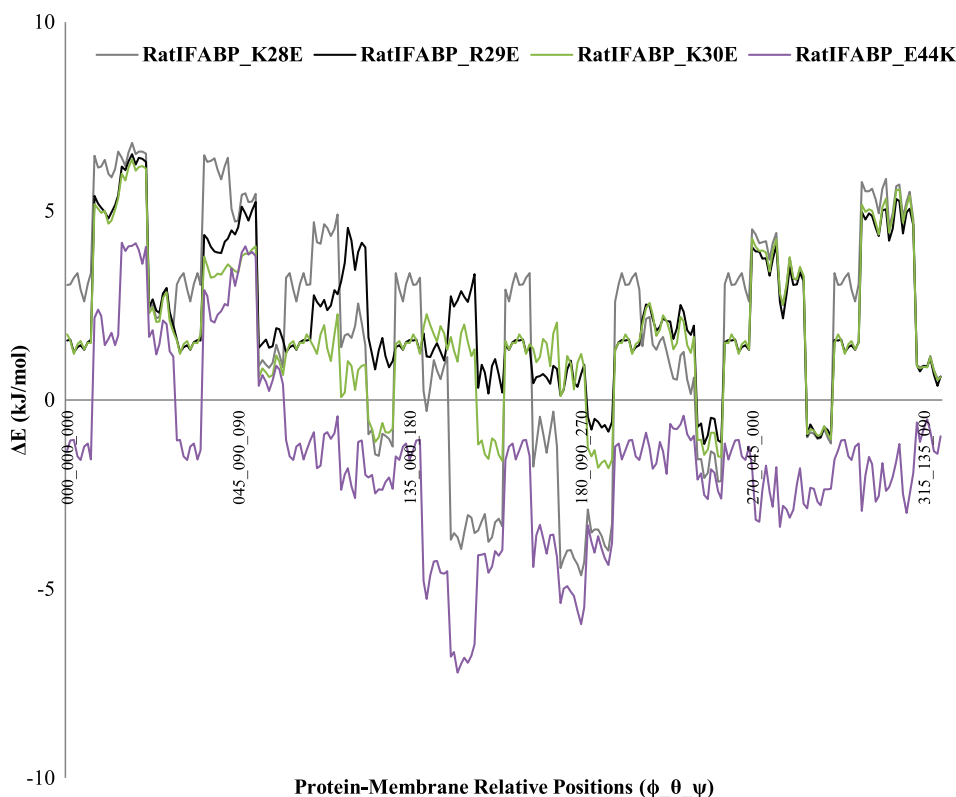
Figure 5.   Electrostatic free energy versus 256 different configurations of mutated rat IFABPs-membrane complex. For R29E mutated rat IFABP (black line) the profile changes drastically and the minimum disappears; for K30E (green line) similar, although less dramatic results are observed; for K28E (gray line) mutation, results show noticeable changes in the profile, but the minimum electrostatic energy interaction remains at the same relative position than for wild type protein. E44K (purple line) mutation shows a new minimum electrostatic energy interaction for the same relative position than wild type rat LFABP.

3.1.1.   Homology modeling

Regarding validation models, PROCHECK package and RMSD analysis shows that modeled FABPs are robust. For example, Ramachandran plot statistics shows good stereochemical qualities, while RMSD values under 2.000 refer to a low deviation of models from template structures. (Supporting Information Table A).

3.2.   Electrostatic surface analysis

Given the alignment results, and the importance of electrostatics in the interaction mechanism, we decided to mutate conserved charged amino acids located in FABPs surface in regions exposed to the solvent. However, albeit the analysis proposed in this work was carried out in FABPs from different organisms (Table 1), for the sake of clarity we detailed only the results obtained for FABPs from rat.

Results show that a mutation of the most informative amino acids (Arg 29, Lys 30 for Glu and Glu 44 for Lys in rat IFABP. In rat LFABP, Glu 26, Asp 27 for Lys and

Lys 46, 47 for Glu) generates the most significant changes in the equipotential surfaces of both proteins at alpha helix 2 or at the bottom of the beta barrel regions (Figure 3). On the other hand, no significant changes in electrostatics are observed in sensitive areas for mutations on non informative positions (Asp 4, 68, 98 and Lys 17, 21, 93 for rat IFABP. For rat LFABP, Asp 34, Glu 67, Lys 20, 31, 33, 36, 57 and Arg 126. Supporting Information Figure C).

Precisely, in collisional rat IFABP, mutations of residues 29 and 30 (individually and in group) of the alpha helix 2 region, and of negative residues on the region comprehended between residues 40 to 45 (specifically residue 44) at the opposite end of the protein, were considered (Figures 2(a), 3(a) and (b)). In diffusional rat LFABP, negative residues 26–27 were mutated to positive amino acids, and positive residues 46–47 were turned to negative (Figures 2(b), 3(c) and (d)).

The electrostatic energy of interaction with the membrane was then calculated for mutant FABPs, in order to determine if these amino acids are involved in the interaction process.
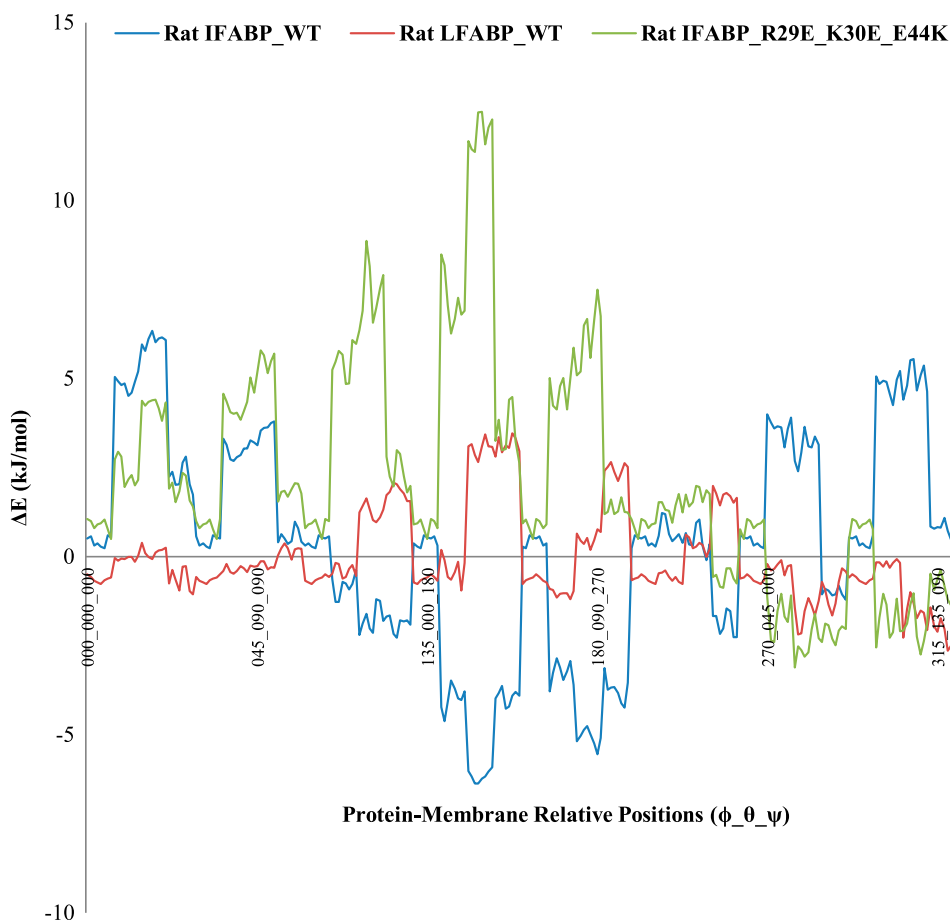
Figure 6.   Key residues in rat IFABP-membrane interaction mechanism. Overlap of wild type rat IFABP (blue line), R29E_K30E_E44K mutant rat IFABP (green line), and wild type rat LFABP (red line). The curves clearly show that these punctual mutations in rat IFABP transform a collisional electrostatic energy profile into a diffusional one.

3.3.   Sampling the electrostatic energy landscape

In a previous work, we showed how FABP-membrane electrostatic potential analysis can predict the interaction mechanisms of a given protein (Zamarreño et al., 2012). As it was shown, electrostatic profile of collisional FABPs shows a defined minimum when alpha helix II is oriented toward the membrane, while for diffusional FABPs, the minimum is not well defined and appears when the bottom of beta barrel is oriented to membrane (Figure 4).

Considering the above, in addition to the high conservation of charged amino acids and the significant change in equipotential surface in mutant proteins, we used APBS in combination with our own software to gain insights into the selection of the FABP-membrane interaction mechanisms. Additionally, we searched for structural features plausibly responsible for the different FABPs-membrane interaction mechanisms. In this way, we calculated the electrostatic energy of interaction

between mutant FABPs and phospholipid membranes as we describe in Materials and Methods.

Considering the high conservation of Arg29 and Lys30 in rat IFABP and that their mutation generate significant changes in the equipotential surfaces, we proposed that these amino acids are fundamental to the minimum energy configuration of the collisional protein. Therefore we calculated the electrostatic energy of interaction with point mutants of one or both amino acids, which resulted in the elimination of the minimum energy configuration. On the other hand, Lys28 (located in the same region) seems to have less influence in the conformation, since its point mutation does not eliminate the minimum energy configuration (Figure 5).

As far as the beta barrel is concerned, the Glu44Lys mutation in rat IFABP results in a new minimum energy configuration that corresponds to the same configuration found in the interaction between rat LFABP and the membrane (Figure 5), showing the relevance of this
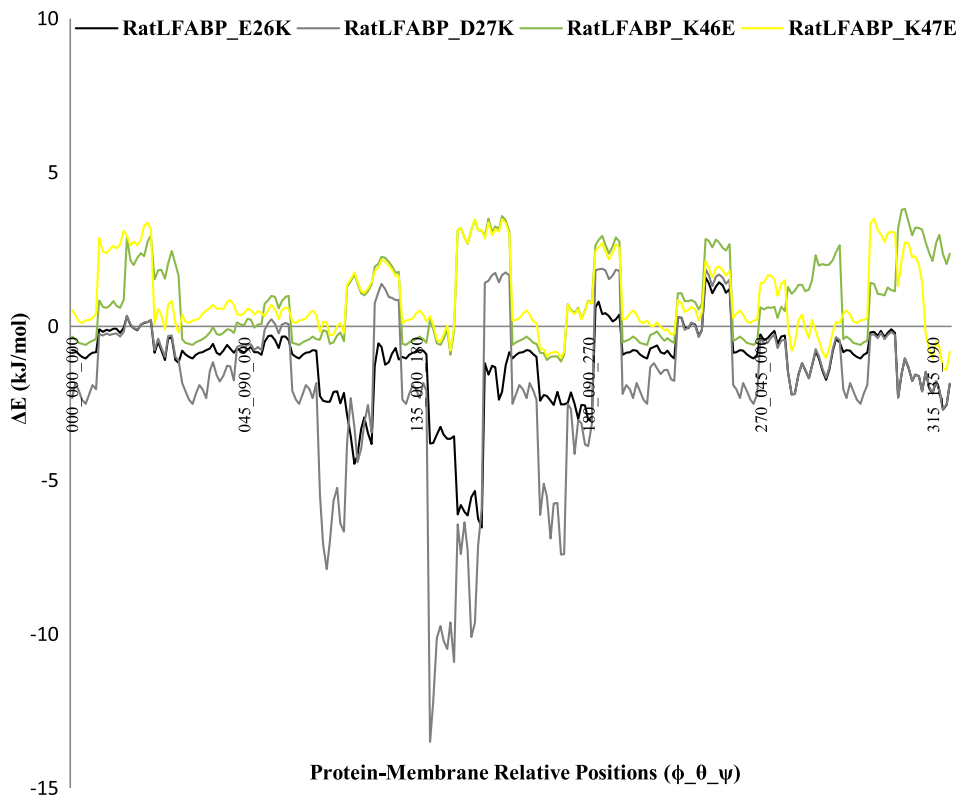
Figure 7.   Electrostatic free energy versus 256 different configurations of rat LFABPs-membrane complex. For E26K mutated rat LFABP (black line) the profile shows transformation of the minimum electrostatic interaction energy into a maximum; for D27K (gray line) similar, even more drastic changes are observed; for K46E (green line) mutation, results show the disappearance of minimum electrostatic energy interaction; mutation K47E (yellow line) shows similar results.

negative residue in the rejection for this relative position. Moreover, combined mutations of only three amino acids (Arg29, Lys30 and Glu44 residues) lead to a reversion of maximum and minimum energy position, resulting in a structure with the same electrostatic features than diffusional rat LFABP and transforming collisional rat IFABP electrostatic profile in a diffusional one (Figure 6).

In the same way, mutation of positively charged residues in positions 29 and/or 30 or equivalent positions, and residue 44 or equivalent for 28 tissue specific collisional FABPs (Table1), seem to indicate that those charged amino acid region as responsible for the collisional electrostatic profile (Supporting Information Figure D I–XII).

For rat LFABP, mutation of negative residues 26 or 27 results in elimination of a maximum energy position, and the formation of a minimum energy position. Also, mutations of Lys46 or Lys47 both for Glu, show a maximum energy position where a minimum energy position for wild type protein was expected (Figure 7). Again, combination of both mutations results in a reversion of maximum and minimum energy position resulting in an electrostatic energy landscape for mutated diffusional

FABP like the one shown for wild type IFABP (Figure 8). Similar results to rat LFABP were obtained for LFABP from the remaining mammal species when highly conserved charged amino acids from alpha helix II were mutated (Supporting Information Figure E I and II). On the other hand, no reversions in electrostatics minimum and maximum were observed in sensitive areas for mutations on non-informative positions (Supporting Information Figure F I–XIV).

3.4.   Molecular dynamics of FABP-membranes first steps interaction

Once minimum and maximum ΔE electrostatic energy for each FABP-membrane relative position was selected, they were used as initial configurations for MD study of FABP-membrane interaction. For each position, mutations of highly conserved residues were made in order to generate a charge inversion. In total, eight MD were carried out, as shown in Table 2. All MD were performed until contact between the protein and the membrane was observed or until the protein was at a significant distance away from the membrane.
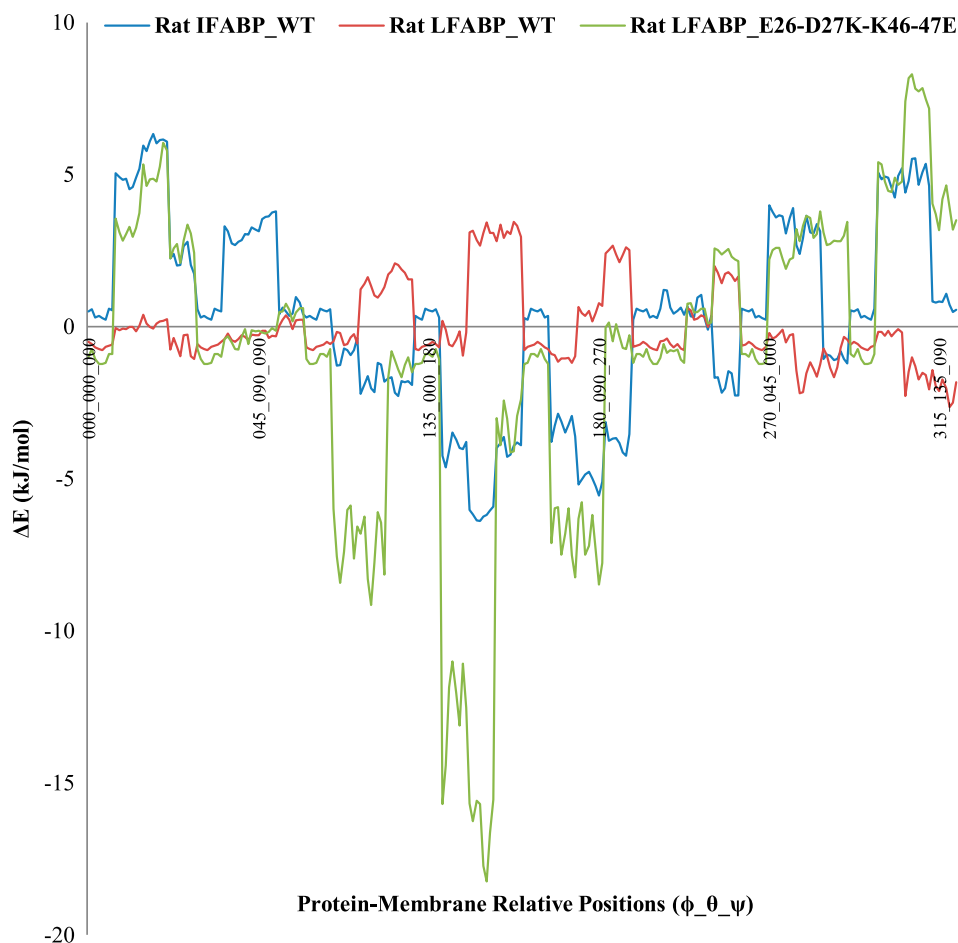
Figure 8. Key residues in rat LFABP-membrane interaction mechanism. Overlap of wild type rat LFABP (red line), E26-D27K_K46-47E mutant rat LFABP (green line), and wild type rat IFABP (blue line). The curves clearly show that these point mutations in rat LFABP transform a diffusional electrostatic energy profile into a collisional one.

Table 2. Summary of MD results.

Protein	Relative position	Mut/WT	MD result
1IFB	Min ΔE, α helix II oriented to membrane	WT	Contact by α helix II
		MUT	No contact recorded
	Max ΔE, β barrel oriented to membrane	WT	No contact recorded
		MUT	Contact by β barrel
2JU3	Min ΔE, β barrel oriented to membrane	WT	Contact by β barrel
		MUT	No contact recorded
	Max ΔE, α helix II oriented to membrane	WT	No contact recorded
		MUT	Contact by α helix II

In those cases where contact between the protein and the membrane was observed, this occurred prior to 10 ns simulation. However, although the objective was only to record the features of the first contact, MD lasted until 100 ns to study the possibility of contact in all cases.

For wild type rat IFABP and LFABP, when MD started in a minimum energy relative position,

FABP-membrane contact was observed (Figures 9 and 10). On the contrary, when the starting relative position was a maximum, no FABP-membrane contact was observed throughout the simulation (Figures 11 and 12). Protein–membrane contact, when observed, starts with a highly conserved charged amino acid, with the only exception of LYS 47 from Rat LFABP. In all cases, these
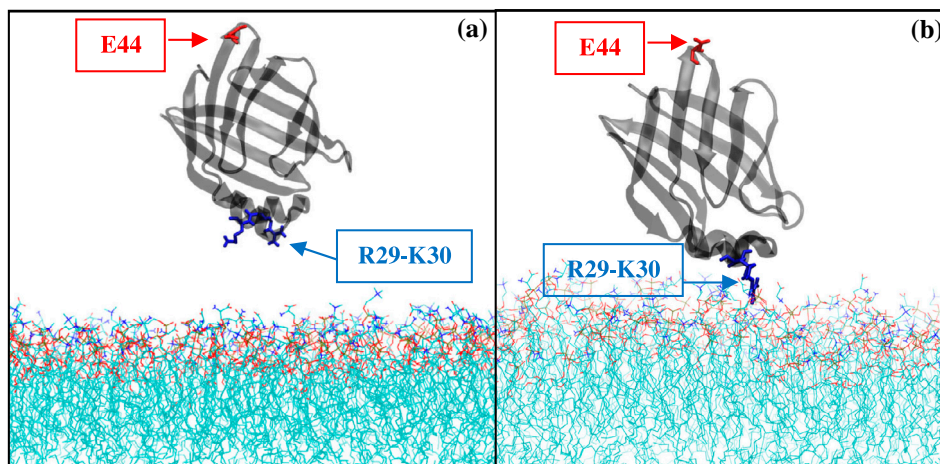
Figure 9. MD of wild type rat IFABP-membrane interaction at minimum electrostatic energy configuration. (a) Snapshot of initial configuration for wild type rat IFABP. Highly conserved positive residues pointing to membrane are shown in blue sticks. Highly conserved negative residues on the opposite side of protein are shown in red sticks. (b) Snapshot of the first step of rat IFABP-membrane interaction. Highly conserved positive residues are the first amino acids to contact the membrane.
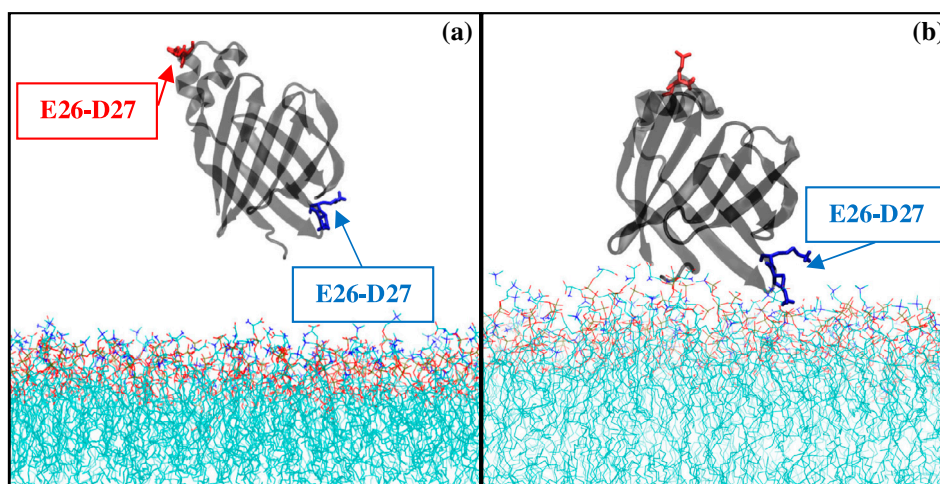

Figure 10. MD of wild type rat LFABP-membrane interaction at minimum electrostatic energy configuration. (a) Snapshot of initial configuration for wild type rat LFABP. Highly conserved positive residues pointing to membrane are shown in blue sticks. Highly conserved negative residues on the alpha helix are shown in red sticks. (b) Snapshot of the first step of rat LFABP-membrane interaction. Highly conserved positive residues are the first amino acids to contact the membrane.

residues were the same that show high relevance in the electrostatic interaction (Figure 13(a) and (b)). Charge reversal of the highly conserved residues induced an opposite behavior to that observed in the WT proteins.

4. Discussion

In this work, we used a computational approach to answer these questions and to gain insight into the process employed. Our analysis allowed us to identify some residues as responsible for the differences.

The results obtained here prompt us to suggest that, in the case of collisional FABPs, the mutation in positively charged residues 29–30 or equivalents, significantly affect the electrostatic profile. Previous experimental work employing point mutants and chimeric proteins demonstrated the importance of charge-charge interaction of the alpha-2 helix of IFABP with membranes and suggests that the charged face of the alpha-2 helix is critical for membrane interactions that lead to the dramatic increase in fatty acid transfer rates from IFABP to anionic membranes (Córsico, Cistola,
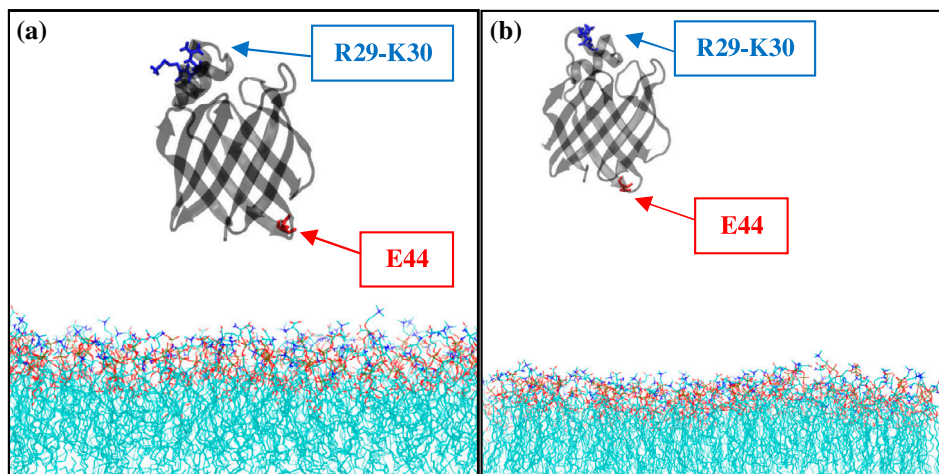
Figure 11. MD of wild type rat IFABP-membrane interaction at maximum electrostatic energy configuration. (a) Snapshot of initial configuration for wild type rat IFABP. Highly conserved positive residues on the opposite side to membrane are shown in blue sticks. Highly conserved negative residues on beta barrel are shown in red sticks. (b) Snapshot of the last ps of MD shows no interaction between rat IFABP and membrane.
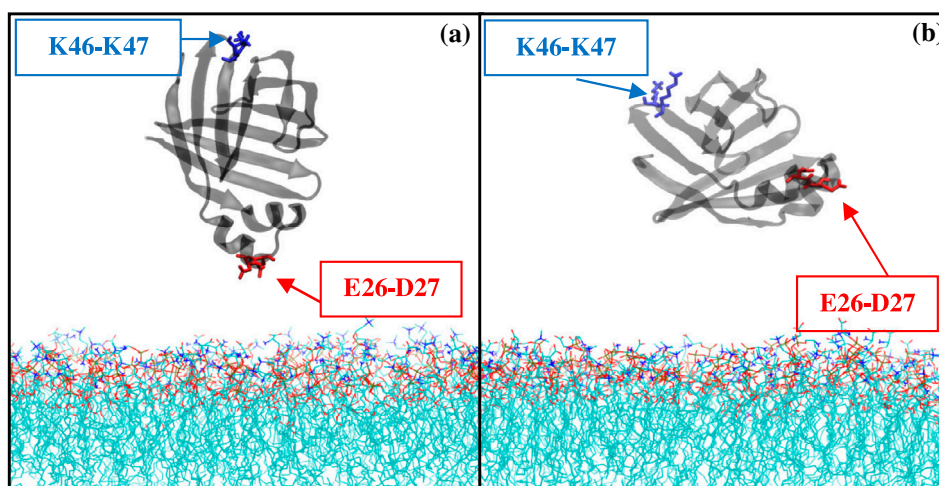

Figure 12. MD of wild type rat LFABP-membrane interaction at maximum electrostatic energy configuration. (a) Snapshot of initial configuration for wild type rat LFABP. Highly conserved positive residues on the beta barrel are shown in blue sticks. Highly conserved negative residues on alpha helix are shown in red sticks. (b) Snapshot of the last ps of MD shows no interaction between rat LFABP and membrane.

Frieden, & Storch, 1998; Córsico, Liou, & Storch, 2004; Córsico et al., 2005; Falomir-Lockhart et al., 2006; Franchini et al., 2008; Sawicki et al., 2014). In addition, mutations in the alpha-2 helix of heart FABP and adipocyte FABP have also demonstrated the participation of alpha-2 in collisional transfer of fatty acids (Herr et al., 1996; Liou & Storch, 2001; Liou, Kahn, & Storch, 2002).

Moreover, the addition of another mutation at negatively charged residue 44 or equivalent in the beta barrel region is able to switch collisional electrostatic profile in to a diffusional one (Figure 6). Similarly, diffusional FABP electrostatic profile could be transformed in a collisional one by mutating just a pair of conserved negative residues located in alpha helix 2, and another pair of positive residues located in the beta barrel region (Figure 8).

On the other hand, MD studies pointed to these highly conserved amino acids as relevant for the interaction, through the fact that these residues are
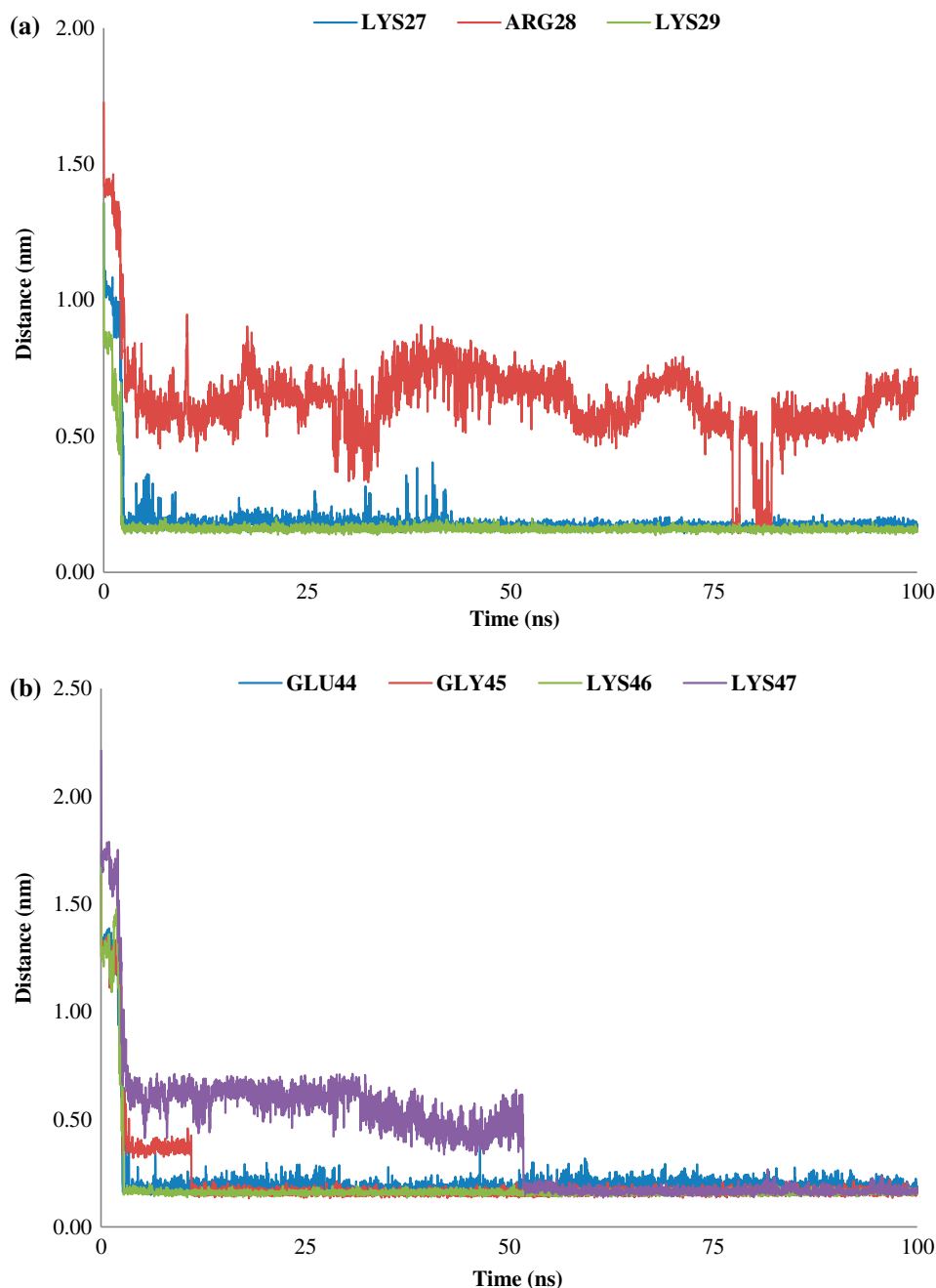
Figure 13.   (a) Distance between highly conserved positive residues of wild type rat IFABP and membrane in MD. Results show that LYS 27 and 29 are the first residues to contact membrane. ARG28 sporadically contacts membrane during simulation. (b) Distance between highly conserved positive residues of wild type rat LFABP and membrane in MD. Results show that LYS 46 is the first residue to contact membrane. Finally, GLU44, GLY 45, and LYS 47 contact the membrane.

involved in the first contact with the phospholipids membrane. Furthermore, the point mutation of charged residues results in a lack of contact between FABP and membrane.

In summary, using computational techniques we characterized the structural determinants of several mammalian FABPs that underlie, in each case, the classification of the proteins as collisional or diffusional and, in that way, their functional features.

To conclude, this computational approach will contribute to predict the behavior of other proteins in their interaction with membranes.

List of Abbreviations

FABPs	Fatty acid binding proteins
SCP2	Sterol carrier protein 2
ACBP	Acyl-CoA binding protein
FA	Fatty acids
MD	Molecular dynamics
POPC	1-palmitoyl-2-oleoyl-phophatidylcholine
SOPS	1-stearoyl-2-oleoyl-phosphatidylserine
APBS	Adaptive Poisson Boltzmann Solver

Disclosure statement

No potential conflict of interest was reported by the authors.

Supplementary material

The supplementary material for this article is available online at http://dx.doi.org/10.1080/07391102.2017.1301271

ORCID

Alejandro Giorgetti http://orcid.org/0000-0001-8738-6150
Marcelo D. Costabel http://orcid.org/0000-0002-8969-7208

References

Baker, N. A., Sept, D., Joseph, S., Holst, M. J., & McCammon, J. A. (2001). Electrostaics of nanosystems: Application to microtubules and the ribosome. *Proceedings of the National Academy of Sciences USA, 98*, 10037–10041. doi:10.1073/pnas.181342398.

Banaszak, L., Winter, N., Xu, Z., Bernlohr, D. A., Cowan, S., & Jones, T. A. (1994). Lipid-binding proteins: A family of fatty acid and retinoid transport proteins. *Advances in Protein Chemistry, 45*, 89–151.

Bass, N. M. (1985). Function and regulation of hepatic and intestinal fatty acid binding proteins. *Chemistry and Physics of Lipids, 38*, 95–114. doi:10.1016/0009-3084(85)90060-X

Berendsen, H. J. C., Postma, J. P. M., van Gunsteren, W. F., & Hermans, J. (1981). Interaction models for water in relation to protein hydration. In B. Piullman Reidel (Ed.), *Intermolecular forces* (pp. 331–342). Dordrecht: Springer Netherlands. doi: 10.1007/978-94-015-7658-1_21

Berendsen, H. J. C., Postma, J. P. M., van Gunsteren, W. F., DiNola, A., & Haak, J. R. (1984). Molecular dynamics with coupling to an external bath. *Journal of Chemical Physics, 81*, 3684–3690. doi:10.1063/1.448118

Berman, H. M., Westbrook, J., Feng, Z., Gilliland, G., Bhat, T. N., Weissing, H., … Bourne, P. E. (2000). The protein data bank. *Nucleic Acids Research, 28*, 235–42. Retrieved from https://www.ncbi.nlm.nih.gov/pmc/articles/PMC102472/

Ceccon, A., Lelli, M., D'Onofrio, M., Molinari, H., & Assfalq, M. (2014). Dynamics of a globular protein adsorbed to liposomal nanoparticles. *Journal of the American Chemical Society, 136*, 13158–13161. doi:10.1021/ja507310m.

Córsico, B., Cistola, D. P., Frieden, C., & Storch, J. (1998). The helical domain of intestinal fatty acid binding protein is critical for colisional transfer of fatty acids to phospholipid membranes. *Proceedings of the National Academy of Sciences USA, 95*, 12174–8. Retrieved from https://www.ncbi.nlm.nih.gov/pmc/articles/PMC22804/

Córsico, B., Liou, H. L., & Storch, J. (2004). The alpha-helical domain of liver fatty acid binding protein is responsible for the diffusion-mediated transfer of fatty acids to phospholipid membranes. *Biochemistry, 43*, 3600–3607. doi:10.1021/bi0357356

Córsico, B., Franchini, G. R., Hjsu, K. T., & Storch, J. (2005). Fatty acid transfer from intestinal fatty acid binding protein to membranes: Electrostatic and hydrophobic interactions. *Journal of Lipid Research, 46*, 1765–1772. doi:10.1194/jlr.M500140-JLR200

Davies, J. K., Hagan, R. M., & Wilton, D. C. (2002). Effect of charge reversal mutations on the ligand- and membrane-binding properties of liver fatty acid-binding protein. *Journal of Biological Chemistry, 277*, 48395–48402. doi:10.1074/jbc.M208141200

Emsley, P., & Cowtan, K. (2004). Coot: Model-building tools for molecular graphics. *Acta Crystallographica, 60*, 2126–2132. doi:10.1107/S0907444904019158.

Eswar, N., Martin-Renom, M. A., Webb, B., Madhusudhan, M. S., Eramian, D., Shen, M., & Pieper, U. (2006). Comparative protein structure modeling with modeller. *Current Protocols in Bioinformatics, 15*, 5.6.1–5.6.30. doi:10.1002/0471250953.bi0506s15

Falomir-Lockhart, L. J., Laborde, L., Kahn, P. C., Storch, J., & Córsico, B. (2006). Protein-membrane interaction and fatty acid transfer from intestinal fatty acid-binding protein to membranes suport for a multistep process. *Journal of Biological Chemistry, 281*, 13979–13989. doi:10.1074/jbc.M511943200

Falomir-Lockhart, L. J., Franchini, G. R., Guerbi, M. X., Storch, J., & Córsico, B. (2011). Interaction of enterocyte FABPs with phospholipid membranes: Clues for specific physiological roles. *Biochimica et Biophysica Acta, 1881*, 452–459. doi:10.1016/j.bbalip.2011.04.005

Franchini, G. R., Storch, J., & Córsico, B. (2008). The integrity of the alpha-helical domain of intestinal fatty acid binding protein is essential for the collision-mediated transfer of fatty acids to phospholipid membranes. *Biochimica et Biophysica Acta, 1781*, 192–199. doi:10.1016/j.bbalip.2008.01.005

Friedman, R., Nachliel, E., & Gutman, M. (2006). Fatty acid binding proteins: Same structure but different binding mechanisms? Molecular dynamics simulations of intestinal fatty acid binding protein. *Biophysics Journal, 90*, 1535–1545. doi:10.1529/biophysj.105.071571

Galassi, V. V., Villarreal, M. A., Posada, V., & Montich, G. G. (2014). Interactions of the fatty acid-binding protein ReP1-NCXSQ with lipid membranes. Influence of the membrane electric field on binding and orientation. *Biochim Biophys. Acta., 1838*, 910–920. doi:10.1016/j.bbamem.2013.11.008

Gilson, M. K., & Honig, B. (1988). Calculation of the total electrostatic energy of a macromolecular system: Salvation energies, binding energies and conformational analysis. *Proteins: Structure, Function and Genetics, 4*, 7–18. doi:10.1002/prot.340040104

Herr, F. M., Aronson, J., & Storch, J. (1996). Role of portal region lysine residues in electrostatic interactions between heart fatty acid binding protein and phospholipid membranes. *Biochemistry., 35*, 1296–1303. doi:10.1021/bi952204b

Herr, F. M., Li, E., Weinberg, R. B., Cook, V. R., & Storch, J. (1999). Differential mechanisms of retinoid transfer from cellular retinol binding proteins types I and II to phopholipid membranes. *Journal of Biological Chemistry, 274*, 9556–9563. doi:10.1074/jbc.274.14.9556

Holst, F. S. M., & Saied, F. (1993). Multigrid solution of the Poisson-Boltzman equation. *Journal of Computational Chemistry, 14*, 105–113. doi:10.1021/ct1006983

Holst, F. S. M., & Saied, F. (1995). Numerical solution of the nonlinear Poisson-Boltzmann equation: Developing more robust and efficient methods. *Journal of Computational Chemistry, 16*, 337–364. doi:10.1002/jcc.540160308.

Hsu, K. T., & Storch, J. (1996). Fatty acid transfer from liver and intestinal fatty acid-binding proteins to membranes occurs by different mechanisms. *Journal of Biological Chemistry, 271*, 13317–23. Retrieved from http://www.jbc.org/content/271/23/13317.long

Jones, D. T., Taylos, W. R., & Thornton, J. M. (1992). The rapid generation of mutation data matrices from protein sequences. *Computer Applications in the Biosciences., 8*, 275–282. doi:10.1093/bioinformatics/8.3.275

Kolafa, J., & Perram, J. (1992). Cutoff errors in the Ewald summation formulae for point charge systems. *Molecular Simulation, 9*, 351–368. doi:10.1080/08927029208049126

Laskowski, R. A., MacArthur, M. W., Moss, D. S., & Thornton, J. M. (1993). PROCHECK – A program to check the stereochemical quality of protein structures. *Journal of Applied Crystallography, 26*, 283–291. doi:10.1107/S0021889892009944

Lee, B., & Richards, F. M. (1971). The interpretation of protein structures: Estimation of static accessibility. *Journal of Molecular Biology, 55*(3), 379–400. doi:10.1016/0022-2836(71)90324-X

Liou, H. L., & Storch, J. (2001). Role of surface lysine residues of adipocyte fatty acid-binding protein in fatty acid transfer to phospholipid vesicles. *Biochemistry, 40*, 6475–6485. doi:10.1021/bi0101042

Liou, H. L., Kahn, P. C., & Storch, J. (2002). Role of the helical domain in fatty acid transfer from adipocyte and heart fatty acid-binding proteins to membranes: Analysis of chimeric proteins. *Journal of Biological Chemistry, 277*(3), 1806–1815. doi:10.1074/jbc.M107987200

Mihalovic, M., & Lazaridis, T. (2007). Modeling fatty acid delivery from intestinal fatty acid binding protein to a membrane. *Protein Science, 16*, 2042–2055. doi:10.1110/ps.072875307

Moult, J., Pedersen, J. T., Judson, R., & Fidelis, K. (1995). A large-scale experiment to assess protein structure prediction methods. *Proteins, 23*, ii–iv. doi:10.1002/prot.340230303

Neves-Petersen, M. T., & Petersen, S. B. (2003). Protein electrostatics: A review of the equations and methods used to model electrostatic equations in biomolecules. *Biotechnology Annual Review, 9*, 315–395. doi:10.1016/S1387-2656(03)09010-0

Pei, J., & Grishin, N. V. (2007). PROMALS: Towards accurate multiple sequence alignments of distantly related proteins. *Bioinformatics, 23*, 802–808. doi:10.1093/bioinformatics/btm017

Poger, D., van Gunsteren, W. F., & Mark, A. E. (2010). A new force field for simulating phosphatidylcholine bilayers. *Journal of Computational Chemistry, 6*, 1117–1125. doi:10.1002/jcc.21396

Pronk, S., Páll, S., Schulz, R., Larsson, P., Bjelkmar, P., Apostolov, R., … Lindajl, E. (2013). GROMACS 4.5: A high-throughput and highly parallel open source molecular simulation toolkit. *Bioinformatics, 29*, 845–854. doi:10.1093/bioinformatics/btt055

Rzepiela, A. J., Schafer, L. V., Goga, N., Risselada, H. J., de Vries, A. H., & Marrink, S. J. (2010). Reconstruction of atomistic details from coarse-grained structures. *Journal of Computational Chemistry, 31*, 1333–1343. doi:10.1002/jcc.21415

Sawicki, L. R., Guerbi, M. X., Falomir-Lockhart, L. J., Curto, L. M., Delfino, J. M., Córsico, B., & Franchini, G. R. (2014). Characterization of fatty acid binding and transfer from Δ98Δ, a functional all-β abridged form of IFABP. *Biochimica et Biophysica Acta, 1841*(12), 1733–1740. doi:10.1016/j.bbalip.2014.09.022

Smith, E. R., & Storch, J. (1999). The adipocyte fatty acid-binding protein binds to membranes by electrostatic interactions. *Journal of Biological Chemistry, 274*, 35325–35330. doi:10.1074/jbc.274.50.35325

Storch, J., & Corsico, B. (2008). The emerging functions and mechanisms of mammalian fatty acid-binding proteins. *Annual Review of Nutrition, 28*, 73–95. doi:10.1146/annurev.nutr.27.061406.093710

Storch, J., & McDermott, L. (2009). Structural and functional analysis of fatty acid-binding proteins. *Journal of Lipid Research, 50*, S126–31. doi:10.1194/jlr.R800084-JLR200

Storch, J., & Thumser, A. E. (2000). The fatty acid transport function of fatty acid-binding proteins. *Biochimica et Biophysica Acta, 1486*, 28–44. doi:10.1016/S1388-1981(00)00046-9

Tamura, K., Stecher, G., Peterson, D., Filipski, A., & Kumar, S. (2013). MEGA 6: Molecular evolutionary genetics analysis version 6.0. *Molecular Biology and Evolution, 30*, 2725–2729. doi:10.1093/molbev/mst197

Thumser, E., & Storch, J. (2000). Liver and intestinal fatty acid-binding proteins obtain fatty acids from phospholipid membranes by different mechanisms. *Journal of Lipid Research, 41*, 647–56. Retrieved from http://www.jlr.org/content/41/4/647.long

Thumser, E., Tsai, J., & Storch, J. (2001). Collision-mediated transfer of long-chain fatty acids by neural tissue fatty acid-binding proteins (FABP): Studies with fluorescent analogs. *Journal of Molecular Neuroscience, 16*, 142–150; discussion 151–157. doi:10.1385/JMN:16:2-3:143

UniProt Consortium (2015). UniProt: A hub for protein information. *Nucleic Acids Research, 43*, 204–212. doi:10.1093/nar/gku989

Villarreal, M. A., Perduca, M., Monaco, H. L., & Montich, G. G. (2008). Binding and interactions of L-BABP to lipid membranes studied by molecular dynamic simulations. *Biochimica et Biophysica Acta, 1778*, 1390–1397. doi:10.1016/j.bbamem.2008.02.015

Waterhouse, A. M., Procter, J. B., Martin, D. M., Clamp, M., & Barton, G. J. (2009). Jalview Version 2-a multiple sequence alignment editor and analysis workbench. *Bioinformatics, 25*, 1189–1191. doi:10.1093/bioinformatics/btp033

Zamarreño, F., Herrera, F. E., Córsico, B., & Costabel, M. D. (2012). Similar structures but different mechanisms: Prediction of FABPs-membrane interaction by electrostatic calculation. *Biochimica et Biophysica Acta, 1818*, 1691–1697. doi:10.1016/j.bbamem.2012.03.003

Zhang, F. C., Lucke Baier, L. J., Sacchettini, J. C., & Hamilton, J. A. (2003). Solution structure of human intestinal fatty acid binding protein with a naturally-occurring single amino acid substitution (A54T) that is associated with altered lipid metabolism. *Biochemistry, 42*, 7339–7347.